Journal of Experimental and Theoretical Physics, Vol. 90, No. 3, 2000, pp. 562–569.
From Zhurnal Éksperimental'noĭ i Teoreticheskoĭ Fiziki, Vol. 117, No. 3, 2000, pp. 644–652.

NONLINEAR PHYSICS

Adiabatic Invariance and Separatrix: Single Separatrix Crossing[¶]

B. V. Chirikov* and V. V. Vecheslavov**

Budker Institute of Nuclear Physics, Siberian Division, Russian Academy of Sciences, Novosibirsk, 630090 Russia
**e-mail: chirikov@inp.nsk.su*
***e-mail: vecheslavov@inp.nsk.su*

Submitted June 22, 1999

Abstract—Detailed numerical experiments on the dynamics and statistics of a single crossing of the separatrix of a nonlinear resonance with a time-varying amplitude are described. The results are compared with a simple approximate theory first developed by Timofeev and further improved and generalized by Tennyson and coworkers. The main attention is paid to a new, ballistic, regime of separatrix crossing in which the violation of adiabaticity is maximal. Some unsolved problems and open questions are also discussed. © *2000 MAIK "Nauka/Interperiodica".*

1. INTRODUCTION

Any conservation law, if only approximate, is of great importance in physics. One of those is the adiabatic invariance that is the conservation of the action variables (J) under a slow parametric perturbation. In the simplest case of a single arbitrarily large variation of the latter, the corresponding change in J is well known to be exponentially small in an appropriate adiabatic parameter ($\epsilon \longrightarrow 0$) provided the perturbation is an analytic function of time or of any other dynamical variable.

However, in the theory of dynamical systems, a much more interesting and important case is a stationary variation of the perturbation (e.g., periodic, quasiperiodic, or even chaotic). In this case, the adiabaticity is violated for sufficiently long length of time, no matter how slow the adiabatic perturbation is. Generic mechanism of such a nonadiabaticity are resonances, both driving and coupling ones, which always determine the long-term dynamics of Hamiltonian oscillator systems. This was first discovered and explained in 1928 by Andronov, Leontovich, and Mandelshtam [1]. Remarkably, it was sufficient, for this purpose, to carefully examine the well-known Mathieu equation and its solutions from the standpoint of physics. Indeed, the instability zones ("stop bands") exist for special but arbitrarily small values of the parameter ϵ, where the adiabaticity is completely destroyed in a sufficiently long length of time. This leads to an additional condition for the adiabatic invariance: the perturbation must be not only slow but also nonresonant.

At a separatrix, an asymptotic trajectory with infinite period of motion, both conditions are violated (see, e.g., [2, 3]). This is exactly the place where the dynamical chaos is born, the ultimate origin of chaos. In a Hamiltonian system, the separatrix is typically associated with nonlinear resonances. The violation of adiabaticity results in the formation of a narrow chaotic layer around the unperturbed separatrix. The set of all resonances is everywhere dense in phase space and forms the so-called "Arnold web." For the number of freedoms $N > 2$ (in a conservative system), a united chaotic component of motion is formed along which a chaotic (but nonergodic!) trajectory is covering the whole energy surface. This very intricate process was termed "Arnold diffusion," which is an universal instability of multidimensional nonlinear oscillations [3–5]. However, the rate of this diffusion, as well as the total measure of the web, is typically exponentially small in perturbation parameter ϵ. For large N or for a driving quasiperiodic perturbation with many frequencies, these nonadiabatic effects decay with ϵ as a power law but only within a finite range $\epsilon_{cr} \lesssim \epsilon \ll 1$ (the so-called fast Arnold diffusion [6]). Asymptotically, as $\epsilon \longrightarrow 0$, the decay is always exponential [7], the crossover value becoming smaller with larger numbers of unperturbed frequencies.

A more serious violation of adiabaticity was found for the crossing of the separatrix by a trajectory. In this case, the change of J is always a power law in ϵ, and, moreover, the measure of the chaotic component does not depend on ϵ at all and is always large. This is true for the slow resonance crossing [8, 9] as well as for the crossing of a single separatrix [9–13]. Interestingly, for the linear oscillator with the frequency value crossing zero, the change of J may be largely independent of ϵ [14].

In this paper, we present the results of numerical experiments for a single crossing of a single separatrix. The present work was stimulated by an interesting

[¶]This article was submitted by the authors in English.

study of the corresponding quantum adiabaticity [15]. We use the same classical model described in the next section.

2. MODEL

The model in [15] we use here is determined by the Hamiltonian

$$H(x, p, t) = \frac{p^2}{2} + A_0 \sin(\omega t)\cos x = \frac{p^2}{2} + \frac{A_0}{2}[\sin(x+\omega t) - \sin(x-\omega t)]. \quad (2.1)$$

The first expression describes a single nonlinear resonance in the pendulum approximation (see, e.g., [3, 5]) with a time-varying amplitude

$$A(t) = A_0 \sin(\omega t). \quad (2.2)$$

Alternatively, the model represents the interaction of two stationary resonances (the second expression in (2.1)) as suggested in [16, 17]. In the latter case, the formal resonance overlap parameter [5]

$$s = \frac{(\Delta p)_r}{\omega} \quad (2.3)$$

indefinitely increases as $\omega \longrightarrow 0$. Here, $(\Delta p)_r$ is the width of each resonance and 2ω is the distance between them. The adiabatic limit $\omega \longrightarrow 0$ corresponding to infinite resonance overlap was suggested in [17] as a new paradigm of "pure" chaos. However, this chaos is generally not ergodic.

Below, we keep to the first interpretation of the model as a single pulsating nonlinear resonance.

The dimensionless adiabaticity parameter is defined in the usual way as the ratio of perturbation/oscillation frequencies. Actually, we can introduce two such parameters:

$$\epsilon = \frac{\omega}{\sqrt{A_0}} \text{ and } \tilde{\epsilon} = \frac{\omega}{\sqrt{|A(t)|}}. \quad (2.4)$$

Here, $\sqrt{A_0}$ is a constant frequency of the small resonance oscillation for the maximal amplitude while $\sqrt{A(t)}$ is the current frequency, particularly at the instant of separatrix crossing. Correspondingly, we call ϵ the global parameter of adiabaticity, and $\tilde{\epsilon}$ the local one.

Two branches of the instant, or "frozen," separatrix at some t = const is defined by the relation

$$p_s(\tilde{x}; t) = \pm 2\sqrt{|A(t)|}\sin(\tilde{x}/2), \quad \tilde{x} = \begin{cases} x, & A(t) > 0, \\ x - \pi, & A(t) < 0. \end{cases} \quad (2.5)$$

Following previous studies of the separatrix crossing, we restrict ourselves to this frozen approximation in what follows. As we shall see, the latter provides quite good accuracy of rather simple theoretical relations.

In this approximation, the action variable is defined in the standard way as

$$J = \frac{1}{2\pi}\oint p(x)dx, \quad (2.6)$$

where the integral is taken over the whole period for x rotation (off the resonance) and over a half of that for x oscillation (inside the resonance). This distinction is necessary to avoid the discontinuity of J at the separatrix where the action is given by a simple expression

$$J = J_s(t) = \frac{4}{\pi}\sqrt{|A(t)|} \le J_{\max} = \frac{4}{\pi}\sqrt{A_0}. \quad (2.7)$$

At $\omega t = 0 \pmod{\pi}$, the action is $J = |p|$ and the conjugated phase is $\theta = x$. Note that, unlike p, the action $J \ge 0$ is never negative.

It is convenient to set $A_0 = 1$ and to introduce the dimensionless action by the transformation $J/J_{\max} \longrightarrow J$. The crossing region is then the unit interval, and J is simply related to the crossing time $t = t_{cr}$ by

$$|A(t_{cr})| = J^2, \quad 0 \le J \le 1, \quad (2.8)$$

while the adiabaticity parameters become

$$\epsilon = \omega \text{ and } \tilde{\epsilon} = \epsilon/J. \quad (2.9)$$

Numerical integration of the equations of motion for Hamiltonian (2.1) was performed in (x, p) variables using the so-called bilateral symplectic algorithm suggested in [18] and based on the symplectic fourth-order Runge–Kutta method in [19]. A typical number of iterations was ~100 per the minimal motion (oscillation) period 2π. This provides the conservation of the Hamiltonian in extended phase space [3] better than 10^{-6}.

As is well known, the variation of J under an adiabatic perturbation consists of one to two qualitatively different parts: (i) the average action, which is nearly constant between the crossings up to exponentially small corrections and which is of primary interest in our problem, and (ii) the rapid oscillations with the motion frequency (see, e.g., Fig. 7c in [20]). The ratio of the two time scales is $\sim\tilde{\epsilon} \ll 1$, which allows the efficient suppression of the second unimportant part of the J variation by simply averaging $J(t)$ over a long time interval $\sim 1/\epsilon$, the suppression factor being $\sim 1/\tilde{\epsilon} \gg 1$ (fairly large).

3. DYNAMICS OF SEPARATRIX CROSSING: DIFFUSIVE REGIME, $J \gtrsim \epsilon^{1/3}$

To the best of our knowledge, the first analytical estimates for the change in J due to separatrix crossing have been calculated in [11] followed shortly by a more accurate [12] and, later, by a more general [9] approxi-

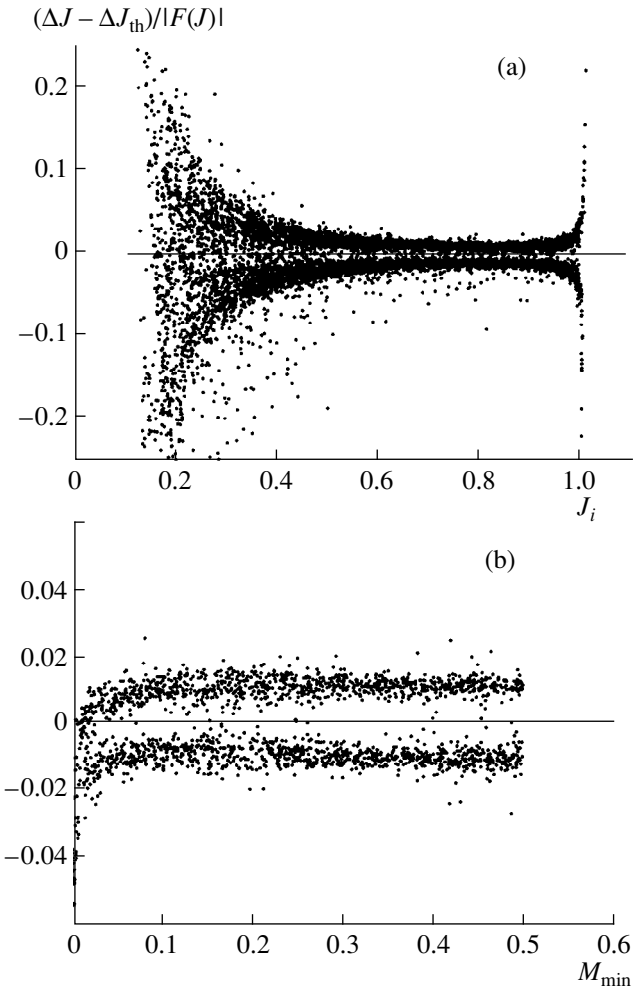

Fig. 1. Normalized deviation of numerical data for separatrix crossings from the simple theory (3.1) in model (2.1): 4 crossings ×2500 trajectories; $\epsilon = 0.001$. (a) Deviation dependence on J in the whole available interval: $0.2 \lesssim J < 1$ (see text). (b) Same data as a function of the crossing parameter M in the best described interval: $0.7 \lesssim J \lesssim 0.9$; accuracy (3.6) $\sigma \approx 0.01$.

mate (asymptotic in ϵ) theory. For model (2.1) under consideration here, these results (see also [21]) can be represented in the form

$$\Delta J(J, M, \epsilon) = F(J)\Phi(M). \tag{3.1}$$

Here, $\Delta J = J_f - J_i$ is the difference between the final and initial averaged values of J.

$$F(J) = -\frac{\epsilon}{2}\frac{\sqrt{1-J^4}}{J^2}\mathrm{sgn}(\dot{A}(t)) \tag{3.2}$$

is the dependence on the averaged action (usually, but not necessarily, the initial one), and

$$\Phi(M) = \ln|2\sin(\pi M)|, \tag{3.3}$$

where M is the "crossing parameter." It looks like a phase canonically conjugated to the action J [21], but it is not. A peculiarity of the separatrix crossing is that the conjugated phase θ cannot even be introduced on the frozen separatrix, because the motion frequency in this approximation is zero, and hence $\theta \equiv$ const. Instead, a different variable, the crossing parameter, is used in the theory [9, 12] determined by any of the following approximate relations:

$$M \approx w_x\frac{A_x^{3/2}}{2\dot{A}_x} \approx w_p\frac{A_p^{3/2}}{4\dot{A}_p} \approx \sin^2\left(\frac{\tilde{x}_s}{4}\right). \tag{3.4}$$

Here,

$$w_x = \frac{|\delta H(t_x)|}{A_x(t_x)}, \quad w_p = \frac{|\delta H(t_p)|}{A_p(t_p)} \tag{3.5}$$

are the closest dimensionless approaches of the trajectory to the unstable fixed point ($\tilde{x} = 0 \pmod{2\pi}$, $p = 0$) just before or after separatrix crossing at time t_x and t_p, respectively (for details, see [9, 12]). The absolute values are assumed for all quantities with subscripts. In the latter expression (3.4), the coordinate $\tilde{x}_s(t_{cr})$ is taken at the instant t_{cr} of separatrix crossing.

The physical meaning of seemingly complicated (3.4) is actually very simple: the main change in J occurs only at the closest approach to the unstable fixed point where the motion is very slow, allowing for the moving separatrix to considerably push or pull the trajectory along. The existing theory cannot distinguish between the three relations (3.4) with respect to their accuracy. However, our numerical experiments revealed that, taken by itself, the third relation ($M = M_3$) proved to be most accurate. On the other hand, if we make use of the first two and take the minimal one of them ($M = M_{\min} \le 0.5$), the accuracy further increases. In this case, it is important to take all the quantities at the corresponding instants t_x and t_p as indicated in (3.4) and (3.5), and not, e.g., at the crossing time t_{cr}. All quantities in (3.4) and (3.5) were computed using the linear interpolation over a single numerical iteration.

A comparison between the numerical results and the simple theory is presented in Fig. 1.

The empirical data (points) represent four separatrix crossings over one period of the adiabatic perturbation $A(t)$ in (2.1) for each of the 2500 trajectories with random initial conditions in the full interval of $\theta = x = (0, 2\pi)$ and of $J = \pi p/4 = (0, 1)$ at $t = 0$. The normalized deviation from the theory is presented as a function of initial $J = J_i$ (prior to a crossing) and of parameter M. In both cases, the optimal $M = M_{\min}$ is used. The best accuracy of the theory roughly corresponds to the interval $0.7 \lesssim J \lesssim 0.9$ (Fig. 1a). The latter is separately shown in Fig. 1b. Beyond this interval, the deviation increases at both sides.

For $J \longrightarrow 1$, the change in J becomes very small (3.1), which increases the theoretical errors. More interesting is the opposite limit ($J \longrightarrow 0$) where the theory becomes singular. It simply means that such a the-

ory is no longer applicable here. This new and interesting region of maximal nonadiabaticity will be considered in Section 4 below. Here we notice only that the absence of any points for $J \lesssim 0.2$ in Fig. 1a has a very simple explanation: using the best parameter, $M = M_{\min}$ becomes inapplicable in this region, because only one of the two close approaches remains here while the other one is never realized. If, instead, one uses a less accurate parameter $M = M_3$, which is always applicable, the deviations exceed 1, which means that the theory (3.1) has nothing to do with such a small J.

The highest accuracy achieved in our numerical experiments $\sigma \approx 0.01$ (see (3.6) and Fig. 1b) is comparable with the minimal theoretical errors $\sim \epsilon \ln \epsilon$ [9]. In a very narrow interval of $M_{\min} \approx 0$, the accuracy becomes somewhat worse but is still surprisingly good for such a simple theoretical relation as (3.1). A few points in this region are clearly seen also in Fig. 1a scattered over a wide interval in J.

The high numerical accuracy achieved reveals a complicated structure of the deviations from the theory. Besides irregular scattering of the points, there is a clear regular "splitting" symmetric with respect to zero deviation, which is determined by the sign of $A(t)$. It might be a result of insufficient J averaging (for discussion see [12]). These regular deviations could be excluded by the explicit computation of the first correction to the adiabatic invariant (2.6) as in [10]. However, it would hardly decrease appreciably the deviations, as they are already of the order of the terms omitted in the theory. In any event, we included this "splitting" in the definition of the accuracy of our numerical data in Fig. 1b for all of the four successive separatrix crossings:

$$\sigma^2 = \frac{\langle (\Delta J - \Delta J_{th})^2 \rangle}{F^2}. \tag{3.6}$$

Here, ΔJ is the empirical and ΔJ_{th} is the theoretical (3.1) value of the J change per crossing.

Another way to demonstrate agreement (or disagreement) of the existing theory with the empirical data is to look at the behavior of the transform

$$\Delta J \longrightarrow (\Delta J)^+ = -\Delta J \operatorname{sgn}(\dot{A}(t)). \tag{3.7}$$

As far as the relation (3.1) holds true, this new quantity has a strict upper bound

$$(\Delta J)^+ \le |F(J)| \Phi(1/2). \tag{3.8}$$

The results are shown in Fig. 2a.

The upper bound of points closely follows the theoretical dependence (3.8) down to $J_i \approx 0.2$ (cf. Fig. 1a). Remarkably, for small J_i, a clear upper bound also exists even though the unknown underlying dynamics is apparently completely different here. In particular, the upper bound in this region does not depend on J and forms a characteristic "plateau." The crossover between the two regions in Fig. 2a is at $J = J_{cro} \approx 0.1$ and scales as $J_{cro} \sim \epsilon^{1/3}$ (see (4.5) below). We shall call the well-understood behavior for $J \gtrsim J_{cro}$ the diffusive region and the other domain $J \lesssim J_{cro}$, to be considered in some detail below, the ballistic region, for reasons explained in the next section.

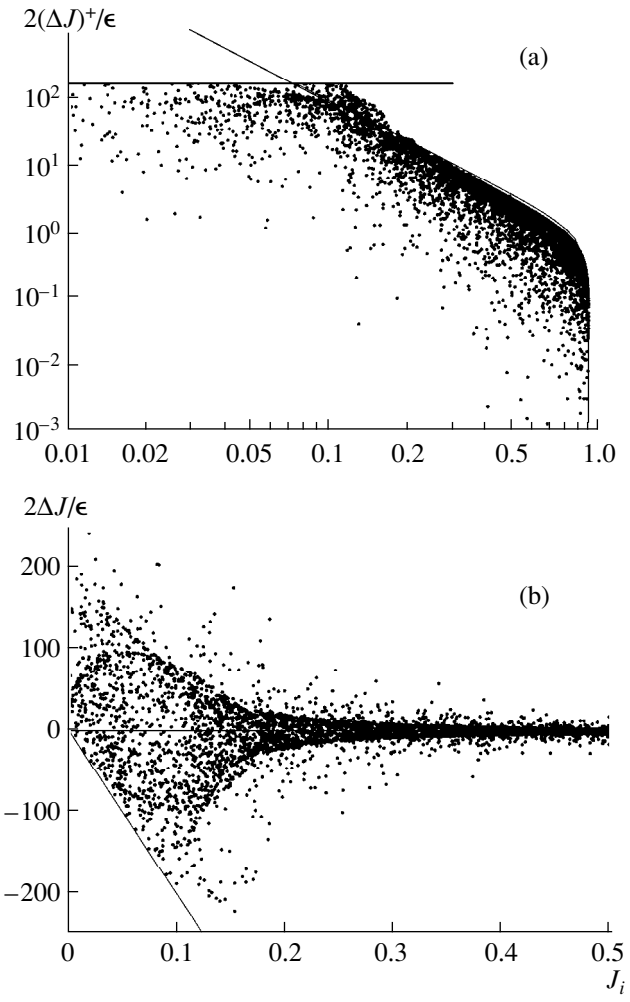

Fig. 2. The set of empirical ΔJ for the ensemble of trajectories as in Fig. 1 in the full range $J_i = (0, 1)$. (a) Transformed quantity $(\Delta J)^+$, (3.7); the solid curve is theory (3.8) shifted upwards by 20%; the horizontal line is empirical upper bound $2(\Delta J)^+/\epsilon \approx 150$ in the region where there is as yet no theory; crossover action $J_{cro} \approx 0.1$. (b) Actual ΔJ with correct signs: the oblique straight line is empirical lower bound $\Delta J \ge -J_i$ (see text).

4. STATISTICS OF SEPARATRIX CROSSING: BALLISTIC REGIME, $J \lesssim \epsilon^{1/3}$

For small $J \lesssim \epsilon^{1/3}$, not only is there the complete absence of any theory, but also constructing the empirical relations seems to us a hard task. Particularly, as is seen in Fig. 2b, the structure in this region is rather complicated.

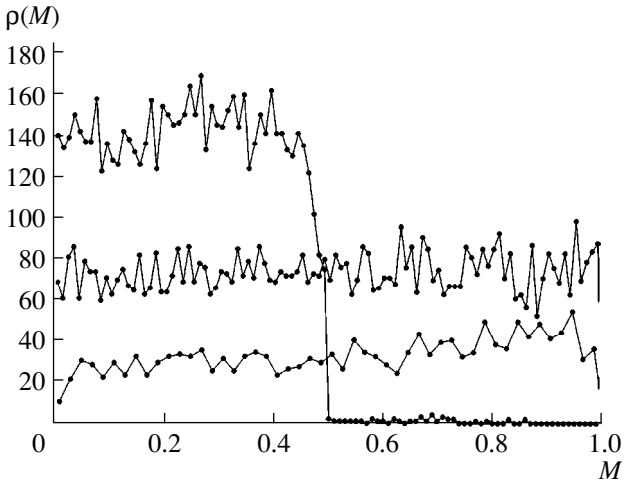

Fig. 3. Distribution $\rho(M)$ in number of crossings per bin: $\epsilon = 0.01$; $J_{cro} = 0.215$. Top to bottom: (i) $M = M_{\min}$, $J_i = (0.3,\ 1)$, the diffusive region, 6928 crossings, 100 bins; (ii) same for $M = M_3$, 7312 crossings; (iii) $M = M_3$, $J_i = (0,\ 0.2)$, the ballistic region, 1634 crossings, 50 bins.

Surprisingly, statistical properties here turned out to be fairly simple. To our knowledge, Mirbach was the first to study this problem numerically in 1998 [22].

Since, in this paper, the properties of the single separatrix crossings are considered, we need a statistical ensemble of trajectories before we turn to statistical numerical experiments. As the motion driven by separatrix crossing is known to be ergodic, or at least very close to that, within the crossing domain, it would be natural to make use of the ergodic ensemble. In this case, the distribution of the crossing parameter M in (3.1), which determines all the statistical properties of the single separatrix crossing, was shown to be homogeneous [9, 23]. Particularly, the two first moments of the M-distribution are

$$\mu_1 = \langle \Phi(M) \rangle = 0,$$
$$\mu_2 = \langle \Phi^2(M) \rangle = \frac{\pi^2}{12}. \tag{4.1}$$

Both numerical values hold in the diffusive region only. Moreover, it is insufficient to fix initial J_0 even for the full range of $\theta_0 = (0,\ 2\pi)$. For homogeneous M-distribution, the width of initial distribution $\Delta_0 J_0$ must exceed some critical value given by a simple approximate relation

$$\frac{\Delta_0 J_0}{J_0} > \epsilon \frac{\sqrt{1 - J_0^4}}{J_0^3} \ln\left(\frac{8}{\epsilon} \frac{J_0^3}{\sqrt{1 - J_0^4}} \right) \approx \frac{J_{cro}^3}{J_0^3} \ln\left(8 \frac{J_0^3}{J_{cro}^3} \right). \tag{4.2}$$

This relation is obtained from the condition that the initial strip $J_0 = (0,\ 1)$ is transformed in such a strip near an unstable fixed point (see (3.1)), which provides the full range of parameter $M = (0.1)$. In most of our statistical numerical experiments, we used the full range of $J_0 = (0,\ 1)$.

In Fig. 3, the M-distribution is shown for both definitions of this parameter.

Two upper distributions in the diffusive region are fairly homogeneous within statistical fluctuations. In contrast, the lower one in the ballistic region shows a clear slope, whose mechanism remains unclear.

The statistical properties we studied are characterized by the two first moments of the distribution function in ΔJ (see (3.1)) defined as follows:

$$(\Delta J)_2^2 \equiv \langle (\Delta J)^2 \rangle = F^2(J)\mu_2 = \frac{\epsilon^2}{4}\left(\frac{1}{J^4} - 1 \right)\mu_2,$$
$$(\Delta J)_1 \equiv \langle \Delta J \rangle = \frac{d}{dJ} \frac{\langle (\Delta J)^2 \rangle}{2} = -\frac{\mu_2 \epsilon^2}{2J^5}. \tag{4.3}$$

Both analytical expressions are valid in the diffusive region only. Moreover, the second one cannot be deduced from the existing first-order theory, as $\langle \Delta J \rangle \sim \epsilon^2$ is a second-order effect. Instead, one can use the well-known relation between the two moments (see, e.g., [3]), which generally holds true for a chaotic Hamiltonian system (for discussion, see [2]). This relation, as well as the second-order moment $\langle \Delta J \rangle$, which may seem to be negligible at first glance, are in fact very important for derivation of the correct diffusion equation

$$\frac{\partial f(J, \tau)}{\partial \tau} = \frac{\partial}{\partial J} \frac{D(J)}{2} \frac{\partial f}{\partial J}. \tag{4.4}$$

Particularly, this equation entails the relaxation to a homogeneous steady state $f(J, \tau) \longrightarrow f_s(J) = \text{const}$ as it should be for the ergodic system.

In (4.4), τ is the discrete time measured in the number of separatrix crossings and $D(J) = \langle (\Delta J)^2 \rangle$ denotes a "diffusion rate" [21, 23]. Actually, this is not the real diffusion rate which includes the correlation between successive crossings. This may be important in the problem under consideration according to numerical data in [21] (for further discussion, see Section 5 below).

The results of our numerical experiments on the statistical properties for a single separatrix crossing are presented in Fig. 4a. We used the same numerical data as in Fig. 2b, which upon ordering in J were averaged by the standard method of the moving window of width of 500 points, or $\Delta_w J \approx 0.05$. The transition from the diffusive to the ballistic regime is surprisingly sharp, especially for $(\Delta J)_1$ (lower curve). The crossover value

$$J = J_{cro} = \alpha \epsilon^{1/3}, \quad \alpha \approx 1.08, \tag{4.5}$$

where empirical factor α was found from the plateau (upper bound) for $(\Delta J)_2$ (upper curve). To this end, we substitute J_{cro} for J in (4.3) to obtain

$$(\Delta J)_2 \le \frac{\sqrt{\mu_2}}{2\alpha^2} \epsilon^{1/3}. \tag{4.6}$$

Remarkably, the empirical data follow with a reasonable accuracy the diffusive theory literally down to the very crossover. This allowed us to numerically discern the very small but important first moment and even to check its agreement with the theory.

Even though there is as yet no theory for the ballistic regime, the underlying physical mechanism of the transition is rather simple and comprehensible [22]. This transition is determined by the kinetics parameter

$$\kappa \sim \frac{(\Delta J)_2}{J} \sim \frac{\epsilon}{J^3} \ll 1, \tag{4.7}$$

which is a reduced dynamical scale in J. The latter strong inequality is a necessary condition for the diffusion approximation to the exact integro-differential kinetic equation to hold; hence, we get the term diffusive region for $J \gtrsim J_{cro} \sim \epsilon^{1/3}$. In the opposite limit ($\kappa \gtrsim 1$), the trajectory jumps over the whole region $\sim J$ in one separatrix crossing. This is usually called the ballistic regime.

Since the action $J \geq 0$ cannot be negative, the change ΔJ is necessarily restricted for any J. In the ballistic region, the restriction becomes very strong, as the strict lower bound in Fig. 2b demonstrates. It simply means that $J_f \geq 0$, as well as J_i. Also, there exists the strict upper bound $J \leq 1$, but it corresponds to a very big ΔJ unless $J \longrightarrow 1$ is close to the upper border of separatrix crossing. Near this border is also the second ballistic region, but its width is very small. Again, it is determined by the kinetics parameter (4.7), which now takes the form

$$\kappa \sim \frac{(\Delta J)_2}{J_1} \sim \frac{\epsilon}{\sqrt{J_1}}, \quad J_1 = 1 - J \tag{4.8}$$

whence a new crossover $J_1^{(cro)} \sim \epsilon^2$.

In the diffusive normalization used in Fig. 4a, the quantities $2(\Delta J)_{1,2}/\epsilon$ do not depend on ϵ in the diffusive region but do so in the ballistic domain. Instead, one may use a different, ballistic, normalization by introducing a new variable $\tilde{J} = J/\epsilon^{1/3}$. The result is presented in Fig. 4b for the two values of ϵ. Instead of (4.3), we now have the relations:

$$(\Delta \tilde{J})_2^2 = \frac{\mu_2}{4}\left(\frac{1}{\tilde{J}^4} - \epsilon^{4/3}\right), \quad (\Delta J)_1 = -\frac{\mu_2}{2\tilde{J}^5}. \tag{4.9}$$

The second one is independent of ϵ in the full range of J. Some difference between the two lower curves is apparently due to fluctuations, especially for the smaller ϵ. The first relation slightly depends on ϵ, but this is important near the upper border ($J \approx 1$) only. The diffusive theory (4.9) is shown in Fig. 4b for $\epsilon = 0.01$ (upper thin curve).

Even though there is as yet no theory for the ballistic region, some statistical properties can be predicted here from a general consideration. One of those is the survival probability $P(\tau)$ for a trajectory to stay in the ballistic region during a time $>\tau$. Namely, this probability is expected to decay exponentially

$$P(\tau) \approx \exp\left(-\frac{\tau}{\langle\tau\rangle}\right) \tag{4.10}$$

with some average survival time $\langle\tau\rangle \sim 1$. This is because, for large jumps of a trajectory across the whole ballistic region, there is a certain probability $w \sim 1$ for a trajectory to remain within this region after each separatrix crossing. Moreover, the successive probabilities are expected, for a chaotic motion, to be equal and

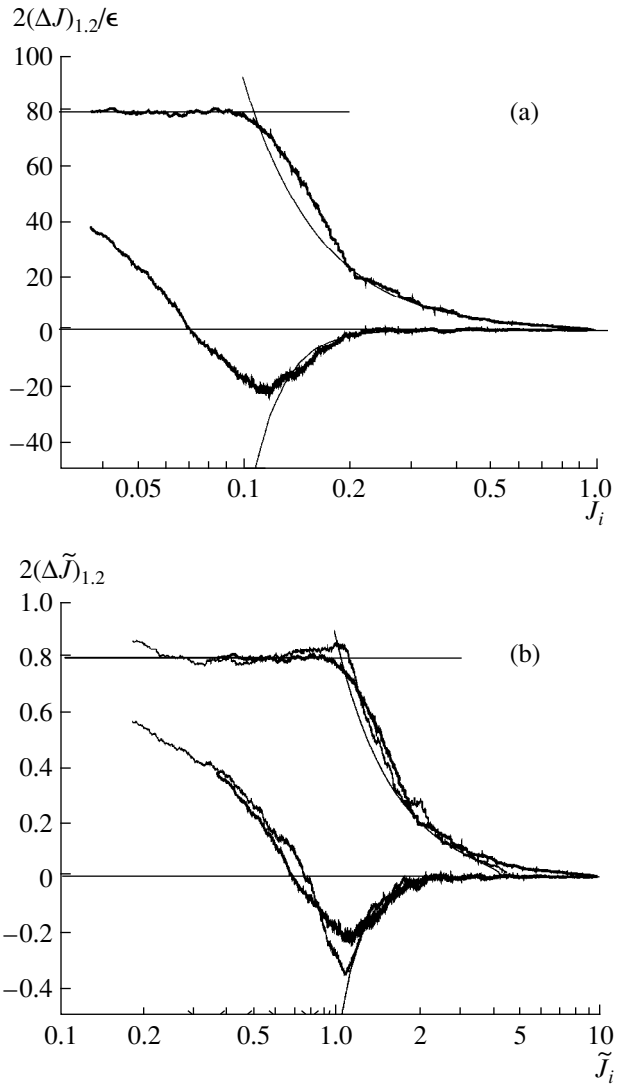

Fig. 4. Statistics of 10^4 separatrix crossings; window width $\Delta_w J \approx 0.05$. (a) $(\Delta J)_2$ (upper thick curve), and $(\Delta J)_1$ (lower curve) vs. J for $\epsilon = 0.001$; two thin solid curves represent the diffusive theory (4.3); the horizontal line is the empirical upper bound for $2(\Delta J)_2/\epsilon \approx 78$. (b) Same data for $\epsilon = 0.001$ and 0.01 in ballistic normalization: $\tilde{J} = J/\epsilon^{1/3}$; empirical upper bound $2(\Delta \tilde{J})_2 \approx 0.78$.

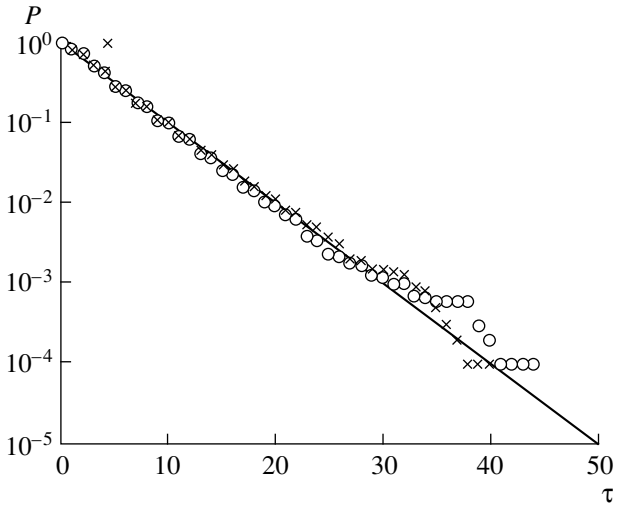

Fig. 5. Survival probability $P(\tau)$ in the ballistic region for $\epsilon = 0.001$ (circles) and $\epsilon = 0.01$ (crosses); 10^4 trajectories homogeneously distributed initially over the ballistic region; the straight line is the fit with $\langle\tau\rangle = 4.35$, $w = 0.79$.

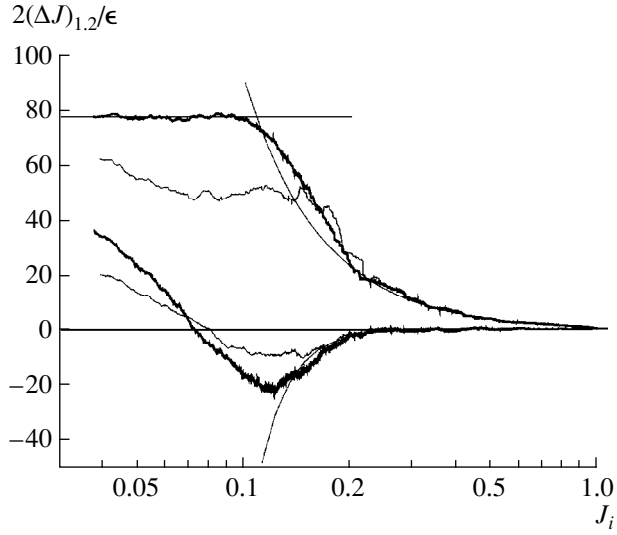

Fig. 6. The effect of correlation over four successive separatrix crossings. Two thick wiggly curves show statistics of the single crossing as in Fig. 4a. Thin wiggly curves represent the effect of fourfold crossings; both moments are normalized (see text).

statistically independent. This implies the exponential (4.10) with $\langle\tau\rangle = -1/\ln w$ independent of ϵ. The latter is especially clear in the ballistic normalization (4.9).

The results of numerical experiments are presented in Fig. 5.

Curiously, the diffusion equation (4.4) with constant $D \approx 0.16$ (in ballistic normalization, see Fig. 4b) also leads to the exponential decay (4.10) with the average survival time

$$\langle\tau\rangle \approx \frac{2}{Dk^2} \approx 5, \qquad (4.11)$$

where $k \approx \pi/2$ is the parameter of the first (main) eigenfunction of the diffusion equation: $f_1(\tilde{J}) \approx \cos(k\tilde{J})$. This is surprisingly close to the empirical value $\langle\tau\rangle \approx 4.4$ (Fig. 5) in spite of the formal inapplicability of the diffusion approximation in the ballistic region!

5. DISCUSSION

In the present paper, we reported the results of extensive numerical experiments aimed at the detailed study of the dynamics and statistics of separatrix crossing in the classical model (2.1). Our work was stimulated by an interesting investigation of the quantum behavior of this model [15].

First of all, we carefully checked the agreement of the empirical data with the existing fairly simple first-order theory [9, 12] and found it surprisingly good, close in fact to the formal limiting accuracy of the theory (Fig. 1). In addition, we were able to discern one second-order effect, the behavior of the first moment $\langle\Delta J\rangle(J)$, which is beyond the theory but very important for the diffusion equation. Our numerical results confirm the expected relation between the two moments (see (4.3) and (Fig. 4)).

On the other hand, we have found that such a nice agreement crudely breaks down in the ballistic region $J < J_{cro} \approx \epsilon^{1/3}$ (Fig. 4), which is qualitatively different from the complementary diffusive region $J > J_{cro}$. The new regime of separatrix crossing was first noticed and partly explained in [22]. It is a peculiarity of model (2.1) in which a pulsating separatrix crosses zero. In many other models studied numerically (see, e.g., [10, 11, 20, 21]), the authors tended to avoid the theoretical singularity at $J \longrightarrow 0$ (3.2). This is more simple, of course, but less interesting. Particularly, the largest violation of adiabaticity ($\Delta J \sim \epsilon^{1/3}$) is reached only in the ballistic region (Figs. 2 and 4).

Even though the dynamical theory in this region seems to be a hard task and has not yet developed the statistical properties of the motion, here it looks rather simple. Surprisingly, even a simplified diffusion equation, which may not hold in the ballistic region, still allows for some reasonably accurate estimates (Fig. 5).

In the present paper, we consider the dynamics and statistics of a single separatrix crossing only. Of course, this is insufficient for the full-scale statistical description of the separatrix crossing. As is well known (see, e.g., [20, 21]), the correlations in multiple crossings are generally very essential. In conclusion of our discussion, we present in Fig. 6 the commutative effect of four successive crossings over one period of the perturbation.

Both moments are normalized as follows: $(\Delta J)_1 \longrightarrow (\Delta J)_1/\tau$; $(\Delta J)_2^2 \longrightarrow (\Delta J)_2^2/\tau \equiv D(\tau)$ where discrete time

$\tau = 4$ is the crossing multiplicity in this case (see (4.3)). In the diffusive region 2, both curves coincide within fluctuations, which means that the correlations, if any, are small over four crossings. This is in agreement with the results in [21] (for a different model). Whether they will rise with τ and why is an interesting and open question. According to [21], they do so, but it may depend on the method of measuring the diffusion rate. In the ballistic region, the correlation effect is strong from the beginning, especially for the second moment. This is also in agreement with numerical data in [22]. According to data in Fig. 6, the normalized second moment (the "diffusion rate") decreases as $D(\tau) \propto 1/\sqrt{\tau}$. What is even more important, the size of the ballistic region grows: $J_{cro}(\tau) \propto \tau^{1/8}$. An intriguing question is whether this trend will continue and, if so, for how long.

ACKNOWLEDGMENTS

We are grateful to Bruno Mirbach, who kindly provided for us his numerical results prior to publication. We appreciate many interesting and stimulating discussions with him and Giulio Casati. This work was partially supported by the Russian Foundation for Fundamental Research, project no. 97-01-00865.

REFERENCES

1. L. I. Mandelshtam, *Complete Works* (Akad. Nauk SSSR, Moscow, 1948), Vol. 1, p. 297.
2. B. V. Chirikov, *Reviews of Plasma Physics*, Ed. by B. B. Kadomtsev (Énergoatomizdat, Moscow, 1984; Consultants Bureau, New York, 1987), Vol. 13.
3. A. Lichtenberg and M. Lieberman, *Regular and Chaotic Dynamics* (Springer, New York, 1992).
4. V. I. Arnold, Dokl. Akad. Nauk SSSR **156**, 9 (1961).
5. B. V. Chirikov, Phys. Rep. **52**, 263 (1979).
6. B. V. Chirikov and V. V. Vecheslavov, J. Stat. Phys. **71**, 243 (1993); Zh. Éksp. Teor. Fiz. **112**, 1132 (1997) [JETP **85**, 616 (1997)].
7. N. N. Nekhoroshev, Usp. Mat. Nauk **32** (6), 5 (1977); P. Lochak, Phys. Lett. A **143**, 39 (1990); Usp. Mat. Nauk **47** (6), 59 (1992); P. Lochak and A. Neishtadt, Chaos **2**, 495 (1992).
8. B. V. Chirikov, Dokl. Akad. Nauk SSSR **125**, 1015 (1959) [Sov. Phys. Dokl. **4**, 390 (1959)]; B. V. Chirikov and D. L. Shepelyanskiĭ, Zh. Tekh. Fiz. **52**, 238 (1982) [Sov. Phys. Tech. Phys. **27**, 156 (1982)].
9. J. Tennyson *et al.*, Phys. Rev. Lett. **56**, 2117 (1986); Phys. Rev. A **34**, 4256 (1986).
10. R. Best, Physica **40**, 182 (1968).
11. R. Aamodt and E. Jaeger, Phys. Fluids **17**, 1386 (1974).
12. A. V. Timofeev, Zh. Éksp. Teor. Fiz. **48**, 1303 (1978) [Sov. Phys. JETP **48**, 656 (1978)].
13. V. Ya. Davydovskiĭ and A. I. Matveev, Zh. Tekh. Fiz. **53**, 2125 (1983) [Sov. Phys. Tech. Phys. **28**, 1302 (1983)]; A. I. Neishtadt, Fiz. Plazmy **12**, 992 (1986) [Sov. J. Plasma Phys. **12**, 568 (1986)].
14. C. Eckart, Phys. Rev. **35**, 1303 (1930); A. S. Bakav and Yu. P. Stepanovsky, *Adiabatic Invariants* (Naukova Dumka, Kiev, 1981).
15. B. Mirbach and G. Casati, Phys. Rev. Lett. **83**, 1327 (1999).
16. C. Menyuk, Phys. Rev. A **31**, 3282 (1985).
17. Y. Elskens and F. Escande, Physica D **62**, 66 (1993).
18. L. Casetti, Phys. Scr. **51**, 29 (1995).
19. E. Forest and R. Ruth, Physica D **43**, 105 (1990).
20. J. Cary and R. Skodje, Physica D **36**, 287 (1989).
21. D. Bruhwiler and J. Cary, Physica D **40**, 265 (1989).
22. B. Mirbach, private communication.
23. J. Cary, F. Escande, and J. Tennyson, Report No. IFSR-155 (Institute for Fusion Studies Report, 1984).